

AD-A037 367

NAVY ELECTRONICS LAB SAN DIEGO CALIF  
ACOUSTIC BOTTOM REFLECTIVITY AT 1.5 KC.(U)  
MAY 63 R R GARNER, W E BATZLER

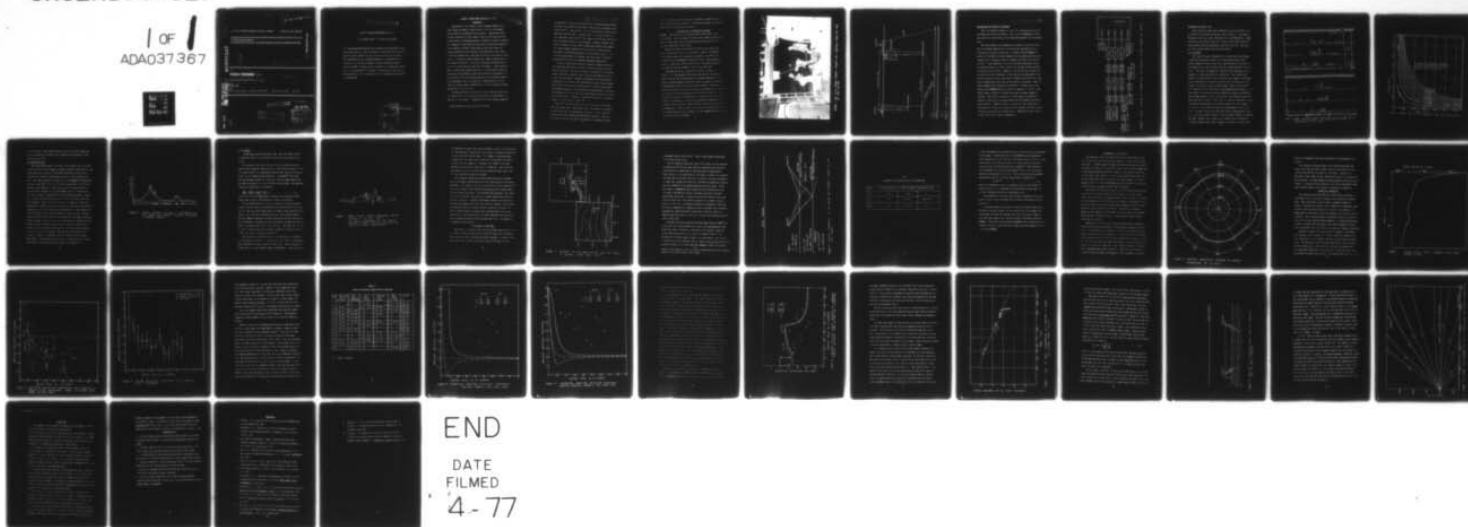
F/G 20/1

UNCLASSIFIED

NEL-TM-603

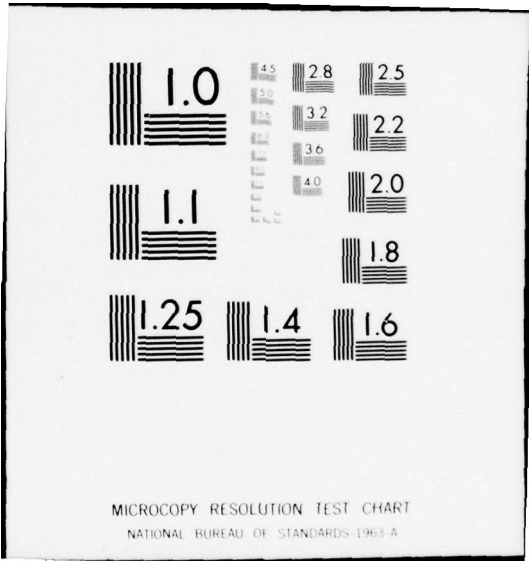
NL

1 OF 1  
ADA037367



END

DATE  
FILMED  
4-77



MICROCOPY RESOLUTION TEST CHART  
NATIONAL BUREAU OF STANDARDS-1963-A

(1) MOST PROJECT 2  
B.S.

U. S. NAVY ELECTRONICS LABORATORY, SAN DIEGO, CALIFORNIA • A BUREAU OF SHIPS LABORATORY

The opinions expressed herein are those of the author(s) and are not necessarily the official views of the U. S. Navy Electronics Laboratory  
If cited in the scientific literature, this document should be described as an unpublished memorandum.

NEL/Technical Memorandum 603

4089

ADA 037367

Good

14 NEL-TM-603

9 TECHNICAL MEMORANDUM TM-603

12 44p

6 ACOUSTIC BOTTOM REFLECTIVITY AT 1.5 KC.

253 550

11 8 May 1963

10 R. R. Garner and W. E. Batzler (Code 3185) SF 001 03 01 (8105) NEL LI-5

DDC FILE COPY

Copy available to DDC does not permit fully legible reproduction

650313-0162

DISTRIBUTION STATEMENT A  
Approved for public release;  
Distribution Unlimited

DDC  
RECEIVED  
MAR 7 1977  
A

TM 603

✓ 1972-2

lpg

BEST AVAILABLE COPY

ACOUSTIC BOTTOM REFLECTIVITY AT 1.5 MC

R. R. Gardner and W. E. Satsler, Code 3185

↳ This memorandum describes the equipment and experimental technique being used in a study of acoustic bottom reflectivity and also presents a small amount of data, obtained on the first sea trip. → (cont on p 20)

This memorandum has been prepared because it is believed that the information covered may be useful to others working on similar problems at NEL. It should not be construed as a formal NEL report since its only purpose is to present information on a small part of NEL Problem LL-5. Only limited distribution outside the Laboratory is contemplated.

SEARCHED BY	INDEXED BY
SERIALIZED BY	FILED BY
FEB 1966	
FBI - NEW YORK	
Litter on file	
DISTRIBUTION STATEMENT CODES	
Dist. STATE OF NEW YORK	
A	23

650313-0162

## ACOUSTIC BOTTOM REFLECTIVITY AT 1.5 KC

### BACKGROUND

Improvement in the design of sonar equipment depends to a large extent on improved understanding of the sea environment and its effect on underwater sound signals. Applications which involve reflection of sound signals from the sea floor have been a particularly troublesome problem in underwater acoustic research. The roughness of the bottom and the depth and physical properties of the layers of sediment which underlie the water layer are usually imperfectly known and may vary considerably even within a relatively small area. Even when the geometry and physical properties of an area are known, predictions, based on theory have not been highly successful. As a result knowledge of bottom reflectivity is usually obtained from field experiments. Recent improvements in theory and improved methods for determining the physical properties of the sediment layers may alleviate this problem. At present however the experimental approach, with increased emphasis on experimental control and accuracy of measurements, is still needed to obtain design information and to test theoretical models appropriate to the situation.

The Rayleigh<sup>1</sup> expression for the bottom reflection coefficient (two-layer case) gives perfect reflection for grazing\* angles less than the critical angle. A modification of this theory, suggested

\* Angle between the sound ray and the bottom.

BEST AVAILABLE COPY

## BEST AVAILABLE COPY

by Mackenzie,<sup>2</sup> considers the effect of the bottom attenuation factor and shows that reflection loss may be expected at all grazing angles greater than  $0^{\circ}$ . The presence of two or more shallow layers of sediment and the existence of sediment layers with sound velocities less than that in the water<sup>3,4</sup> have complicated both the theoretical and experimental aspects of the problem. A number of models considered suitable for deep ocean bottoms have recently been suggested. One of these, suggested by Cole and Bell<sup>5</sup> has been fairly successful in obtaining agreement with experimental results. It is a three-layer model and combines the three-layer solution of Brekhovskikh<sup>6</sup> with the modification suggested by Mackenzie.

Previous experimental studies of acoustic bottom reflectivity have been made with signals of relatively high frequency or with explosive sources. The angle coverage, especially for low grazing angles, has been incomplete. The present study endeavors to give a more complete angular coverage with emphasis on the low angles. Frequencies of 1.5 kc and 10 kc have been used thus far and further tests using 3 kc sources as well as explosive sources are planned. Considerable control of the experiment has been achieved, we believe, by anchoring one or both ships, by using variable depth sources which are non-directional or nearly so, and by the choice of a relatively smooth and level area for a test site.

Data were collected during sea trips in October and December 1961, and August 1962. The present report describes our equipment, the test area, and the experimental procedure. It also presents a portion of the data obtained on the October 1961 trip. This restriction to October 1961 data is a matter of convenience at this

time. Reporting on other data must be delayed to permit study of consistency criteria in all data. The present purpose is to discuss methods with only examples of results.

#### EQUIPMENT AND EXPERIMENTAL PROCEDURE

General: The procedures and equipment used on all three trips were similar. The following description, which refers specifically to the October 1961 trip, will therefore give a general idea of the test procedures for all trips.

Each of the ships (USS REKBURG and YFU-45) was equipped to send, receive and record 1.5 kc underwater signals; the REKBURG also carried radar and echo-sounding equipment. The YFU-45 was anchored while the REKBURG was allowed to drift. The photograph, Figure 1., taken on the YFU-45 shows the 1.5 kc source being put over the bow; the USS REKBURG is seen in the background.

The geometry of the experimental procedure is shown in Figure 2. As the REKBURG drifted away from the YFU, the grazing angle  $\theta$  made by the bottom-reflected ray changed gradually. The number of grazing angles tested was further increased by sending and receiving the sound from several different depths. In general, the sources were kept deep since this avoided troublesome refraction effects and provided low grazing-angle paths from source to receiver. After certain corrections, to be described in a later section, the bottom reflection coefficients could then be obtained by comparing the amplitudes of the direct and bottom-reflected signals as recorded at the receiving ship. Grazing angles were computed by measuring signal transit times from which depths, ranges, and the complete geometry of the test could then be calculated.



FIGURE 1. THE 1.5 Kg SOUND SOURCE RIGGED FOR LOWERING FROM THE BOW OF THE YFU-45

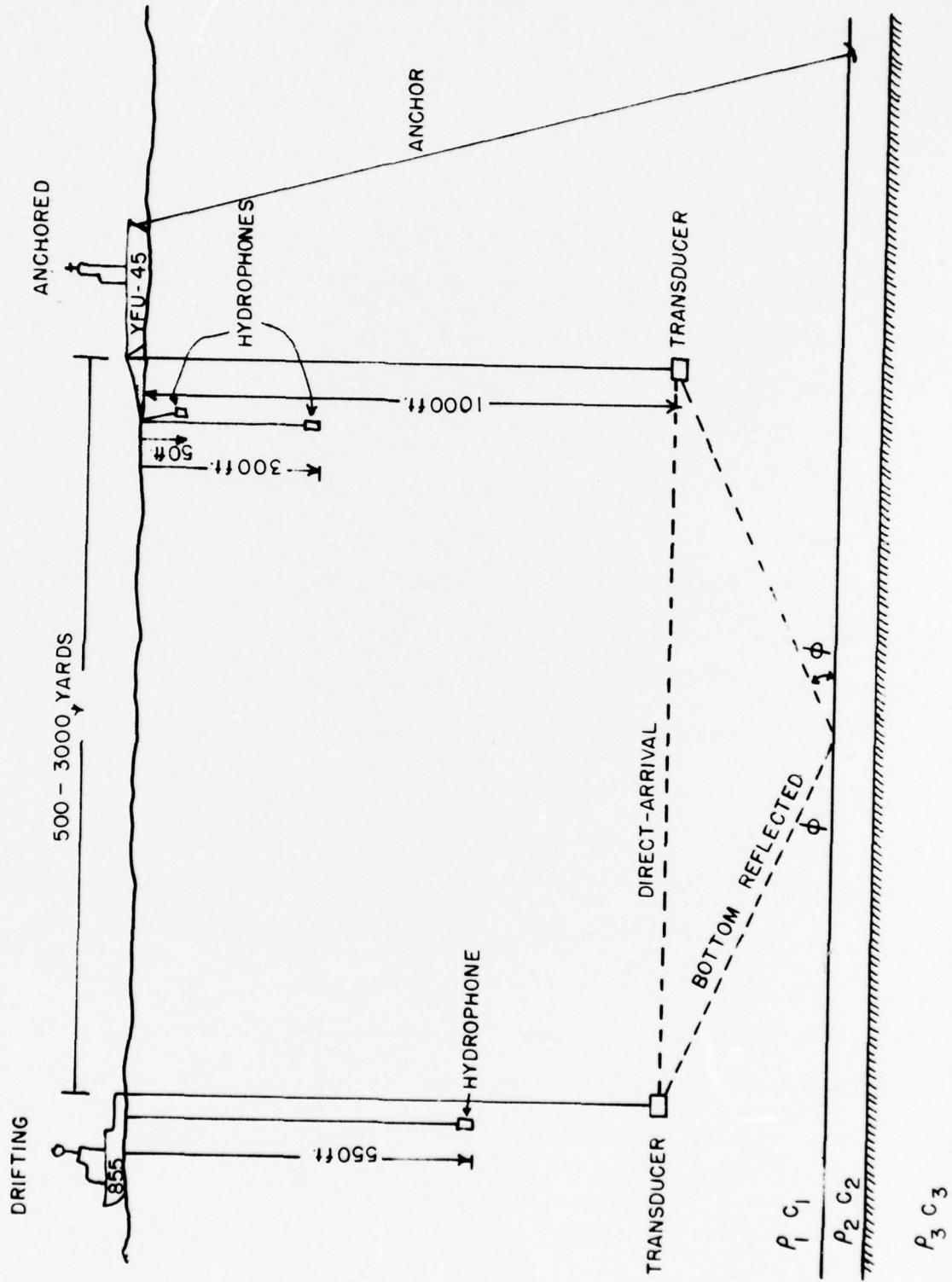


FIGURE 2. GEOMETRY OF EXPERIMENTAL PROCEDURE.

## TRANSMITTING AND RECEIVING EQUIPMENT

The block diagram in Figure 3. shows the transmitting and receiving system used aboard the YFU-45. That on the USS REXBURG was identical except for the addition of the linear FM equipment to be discussed later.

The sound signal to be transmitted originates in the keyer (see Fig. 3) and after amplification is transmitted simultaneously with a radio pulse to the receiving ship. A signal from the REXBURG is received at the YFU-45 on three channels via the shallow and deep hydrophone and the transducer which is normally switched to the receive position. Linear amplifiers (70 db) and variable attenuators bring the received signal to a level suitable for display on three channels of the paper-tape recorder. Channel 1 receives the radio signal which provides a zero-time reference. A 200 cps sine wave generated by the crystal-controlled clock is recorded on channel 5 and serves as a time base for measuring travel time via the various sound paths. Figure 4a shows a sample record obtained on the YFU-45. A 5-msec pulse transmitted by the REXBURG has been received on channels 2, 3 and 4. Each channel shows a number of arrivals which are not always completely resolved. This lack of resolution is clearly shown in Figure 4b, channel 4, where the direct and surface-reflected signals overlap almost completely. Channels 2 and 3 in Figure 4b. show completely resolved direct, bottom, and surface-reflected signals plus other signals resulting from more than one reflections. (Labels B, D and S refer to bottom, direct, and surface, respectively.

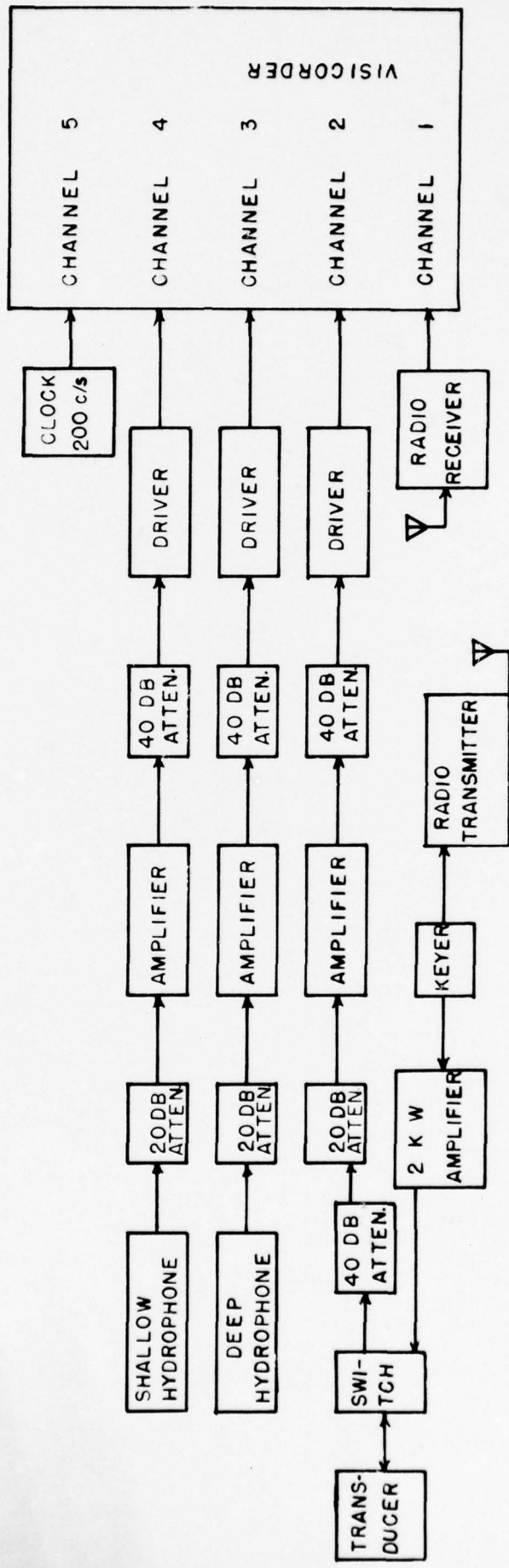


FIGURE 3. BLOCK DIAGRAM OF TRANSMITTING AND RECEIVING SYSTEM ABOARD THE YFU-45

## COMPARISON OF SIGNAL TYPES

Three types of signals were transmitted during the October trip. In addition to the 5-msec CW pulses, seen in Figure 4, two types of FM signals were used; 50-msec FM chirps and linear FM pulses. A major objective of the October trip was to compare these signal types and thus determine the most appropriate type for future use. Each type and their relative merits will now be discussed.

### (1) CW Pulses

The 5 msec CW pulses transmitted at 1.5 kc/s were short enough to give good resolution between the bottom-reflected and direct-arrival signals as long as there was a path difference equivalent to the length of the pulse in water; that is, a path difference of about 8 yds. When these two signals are resolved their amplitudes can be compared to obtain the reflection coefficient. For a given pulse length, the path difference and the grazing angle depend on the separation of the source and receiver and upon their distances above the bottom. The relation between grazing angle, range, and distance of the transducers above the bottom is shown graphically in Figure 5. In this figure it is assumed that both transducers (source and receiver) are the same distance,  $D$ , above the bottom. The X-mark on each curve gives the limit at which a 5-msec pulse is resolved, expressed in terms of range and grazing angle for the given value of  $D$ . For example, if  $D = 100$  yds, usable data is limited to grazing angles of  $\phi=4.5^\circ$  and above. As these curves show, the lower limit to grazing angle coverage using 5-msec pulses is about  $4^\circ$  unless ranges in excess of 3000 yds are used. Shorter pulse lengths will increase this coverage but at 1.5 kc/s a 5-msec pulse, which contains 7.5 cycles, is close to the

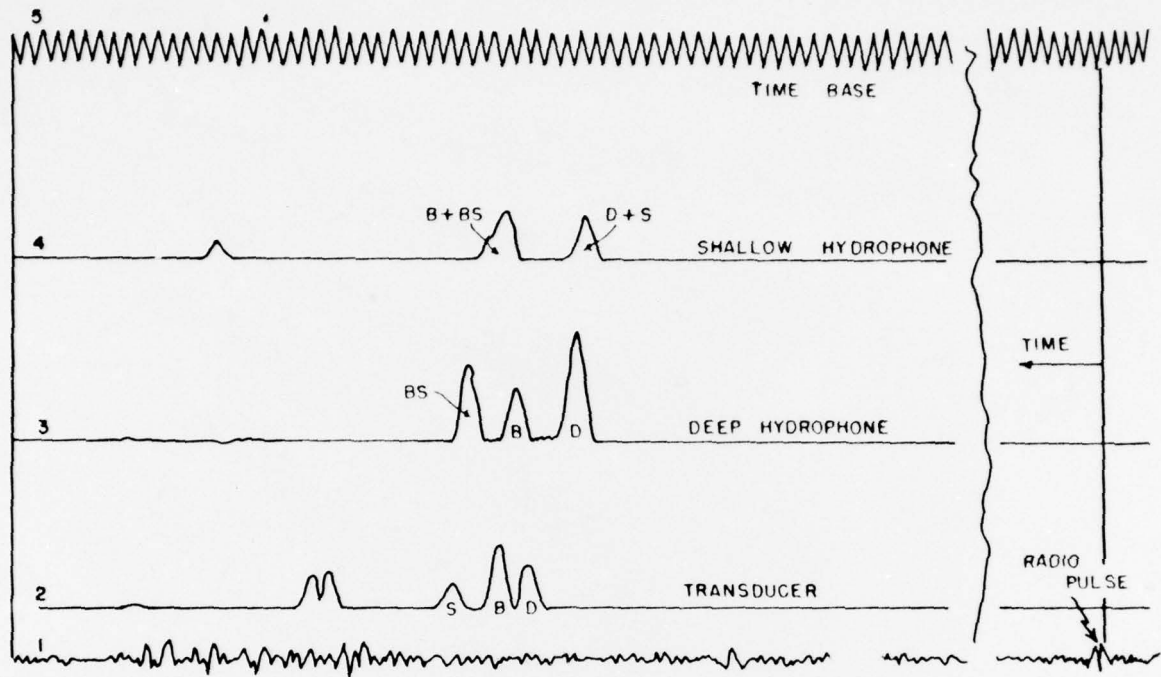


FIG. 4a

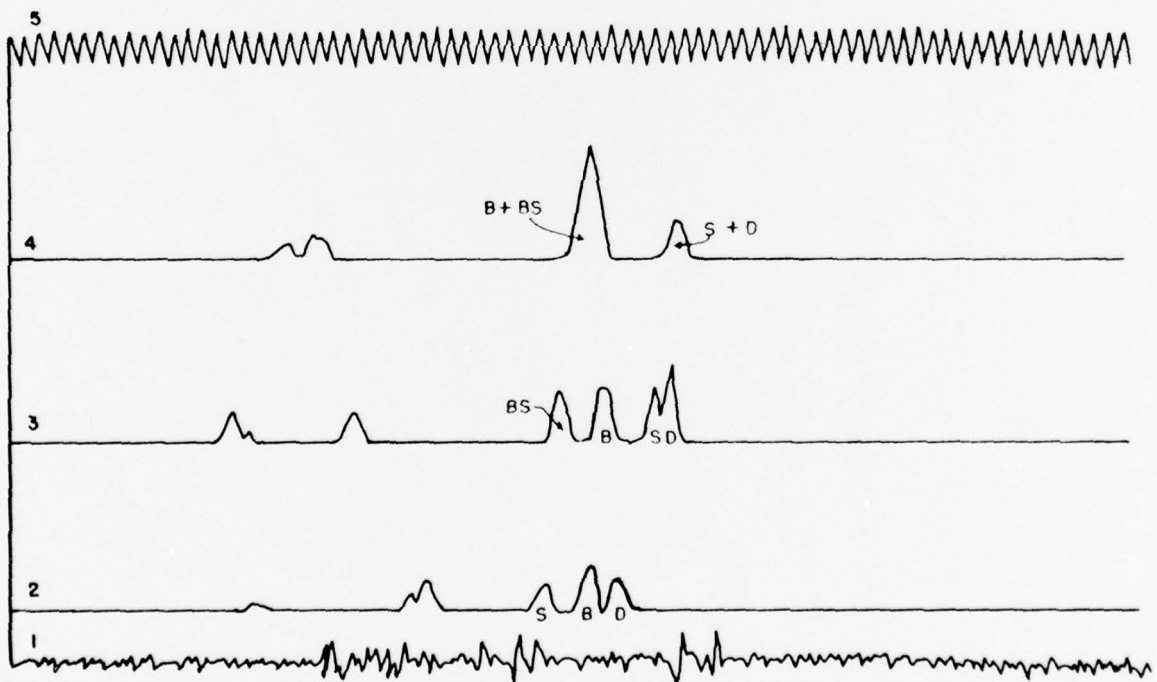


FIGURE 4b. SAMPLE VISICORDER RECORDS SHOWING RADIO PULSE, TIME BASE AND CW PULSE. (D IS DIRECT ARRIVAL, S IS SURFACE-REFLECTED ARRIVAL, BS IS BOTTOM-SURFACE-REFLECTED ARRIVAL.)

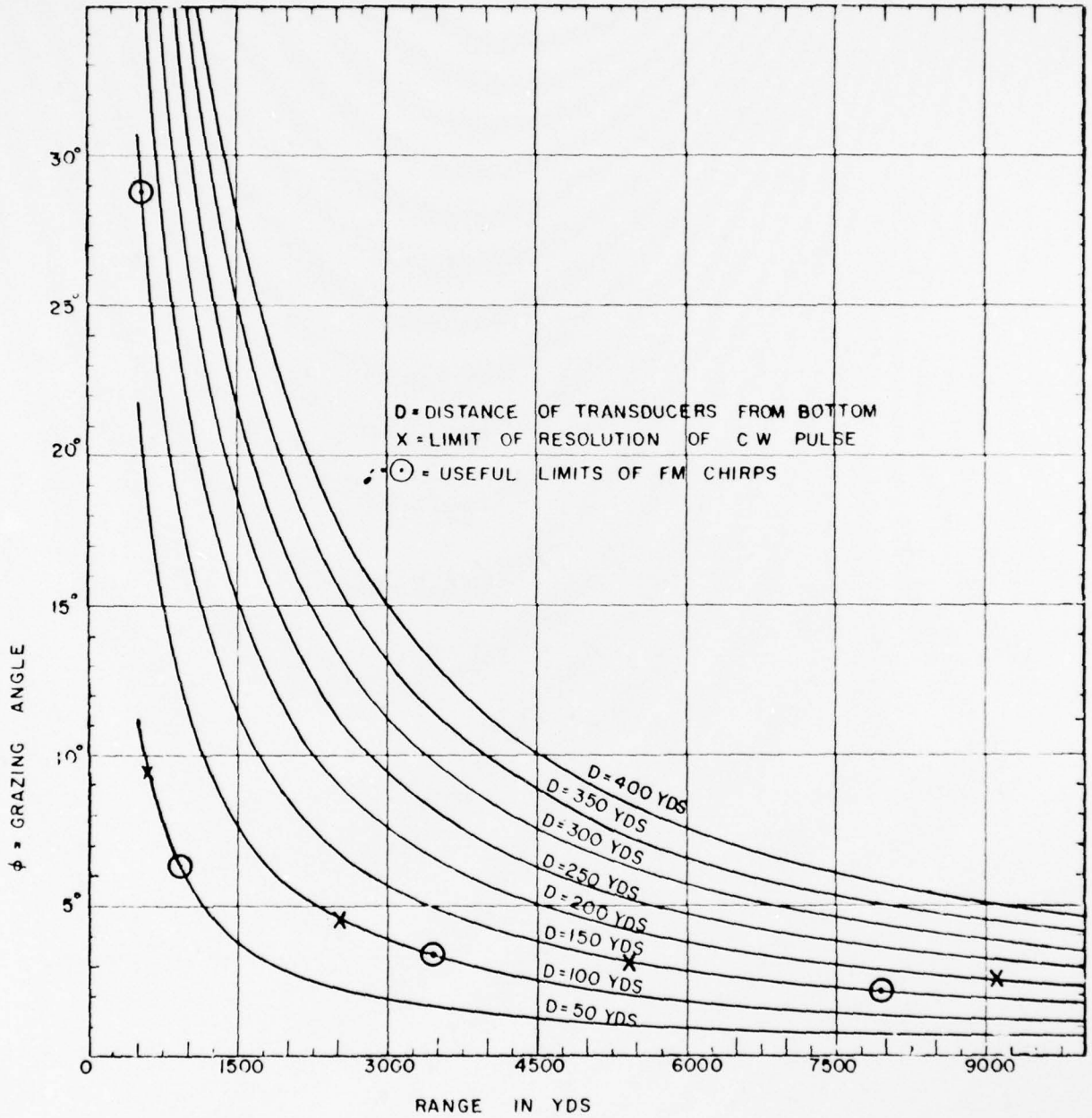


FIGURE 5. GRAZING ANGLE  $\phi$  AS A FUNCTION OF RANGE AND TRANSDUCER DEPTH

practical limit. Interference from the surface reflected signal must also be considered; the same curves, using  $D$  as the distance to the surface, may be used.

## (2) Linear FM Pulses

The linear FM equipment, used only on the October trip, was a modified version of an echo-ranging equipment originally developed for long range, deep-water research.<sup>7</sup> The linear FM pulses were one second long and had a variable sweep frequency with a center frequency of 2 kc/s. The sweep frequency was generated on the REXBURG and transmitted by radio to the YFU-45, where it was then retransmitted into the water through a power amplifier. This expedient was necessary because the only available equipment was on the REXBURG, and it is necessary for the same equipment to generate as well as receive the signals. Figure 6 is a replica of the signals received on the X-Y recorder used with this equipment. After certain corrections, the amplitude reflection coefficient is obtained by finding the ratio between the bottom-reflected amplitude,  $B$ , and the direct-arrival amplitude,  $D$ . This system provided a minimum resolvable path difference of about 10 yds. An upper limit of 185 yds in path difference was imposed by the scale limitations of the recorder. Because the CW pulses were easier to generate and use, because they gave somewhat greater angle coverage, and because they presented fewer calibration problems, the use of the linear FM system in this study was not continued. However, the system worked satisfactorily and may be an important tool for similar studies in deep water where its high signal-to-noise ratio is a more important consideration than in the relatively shallow-water, short-range case.

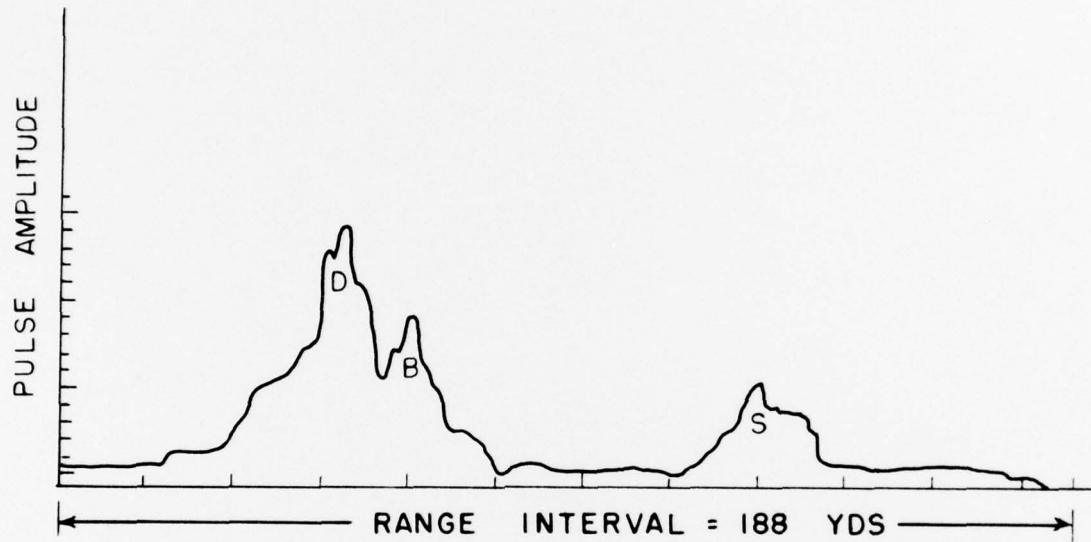


FIGURE 6. SIGNALS RECEIVED ON THE X-Y RECORDER OF THE LINEAR FM SYSTEM. (D= DIRECT, B= BOTTOM, S= SURFACE SIGNALS).

### (3) FM Chirps

The FM chirps used were 50 msec long. They were swept linearly in frequency from 1.3 to 1.6 kc/s at a rate of 6 kc per second, per second.

At a receiver, the sound from the direct and bottom-reflected paths arrives slightly displaced in time. The beating together of the two signals produces an interference pattern which may be seen between B and C in the sample record of Figure 7. Liebermann<sup>8,9</sup> has shown that the maximum reading, M, is the sum of the two signal amplitudes and that the minimum, m, is the difference between them. The amplitude reflection coefficient R is therefore:

$$\frac{M-m}{M+m} = \frac{(d+r) - (d-r)}{(d+r) + (d-r)} = \frac{2r}{2d} = R \dots \dots \dots (1)$$

where d and r are the amplitudes of the direct and reflected signals, respectively, and R is the amplitude reflection coefficient.

Use of the FM chirps is limited to relatively low grazing angles because, for best data, the surface-reflected signal should not arrive until at least one pulse length after the start of the bottom-reflected signal. Also, the path difference must be at least great enough to give one complete maximum and minimum during the time that the signals are interfering. Increasing the path difference increases the beat frequency, thus giving more beats in a given time. The upper limit of useful data is reached when the overlap in signals is just great enough to produce one complete cycle of interference.

When the factors limiting the use of the FM chirp are considered for the present equipment, it is found that useful data is obtained when path differences of from 5.8 yds to 77 yds exist. This corresponds to delay times of 3.6 msec and 46.4 msec, respectively. These limitations

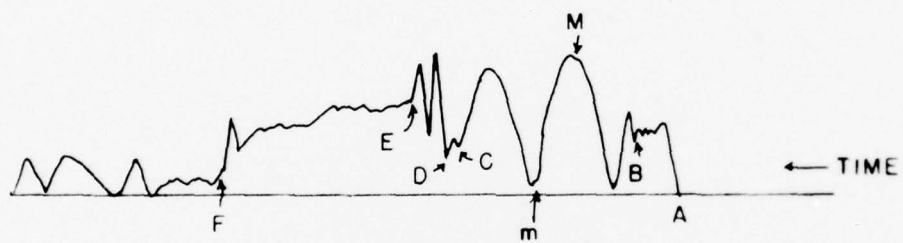


FIGURE 7. SAMPLE RECORD SHOWING INTERFERENCE PATTERN PRODUCED BY AN F M CHIRP.  
 (THE DIRECT, BOTTOM-REFLECTED, AND SURFACE-REFLECTED PULSES BEGIN AT A, B, AND C AND END AT D, E, AND F RESPECTIVELY.)

are indicated on some of the curves of Figure 5 with circles which show the range and angle interval over which useful data may be obtained for a given source and receiver depth. For example, the grazing-angle coverage, when the source and receiver are 150 yds above the bottom, is from a low of 2 degrees to a maximum of 29 degrees; the range interval for this case is from 500 yds to 8000 yds. When the source and receiver are 50 or 100 yds from the bottom the upper angle limit is closer than 500 yds and is not shown.

The increased resolution provided by FM chirps gives somewhat better low-angle coverage than either the 5 msec pulses or the linear FM system. One drawback in the use of the chirps is that ambiguous results are obtained if the bottom reflected pulse has a greater amplitude than the direct pulse. As Liebermann<sup>9</sup> has explained, this ambiguity can be resolved. The process is tedious however and should be avoided if possible. Another disadvantage concerns the necessity for corrections in amplitude because the frequency response of the sources are not flat over the frequency interval covered by the chirp. In spite of these drawbacks further tests with FM chirps will be made since there is some indication of increased stability in results from pulse to pulse and because angle coverage down to 2 or 3 degrees can be obtained by this method.

#### DESCRIPTION OF TEST AREA

The location of the test area off Mission Beach, San Diego is seen in Figure 8. This area was selected because it has a flat moderately deep ocean floor and is readily accessible from NEEL. A further advantage of the site is that it is shallow enough at 200 fms to permit

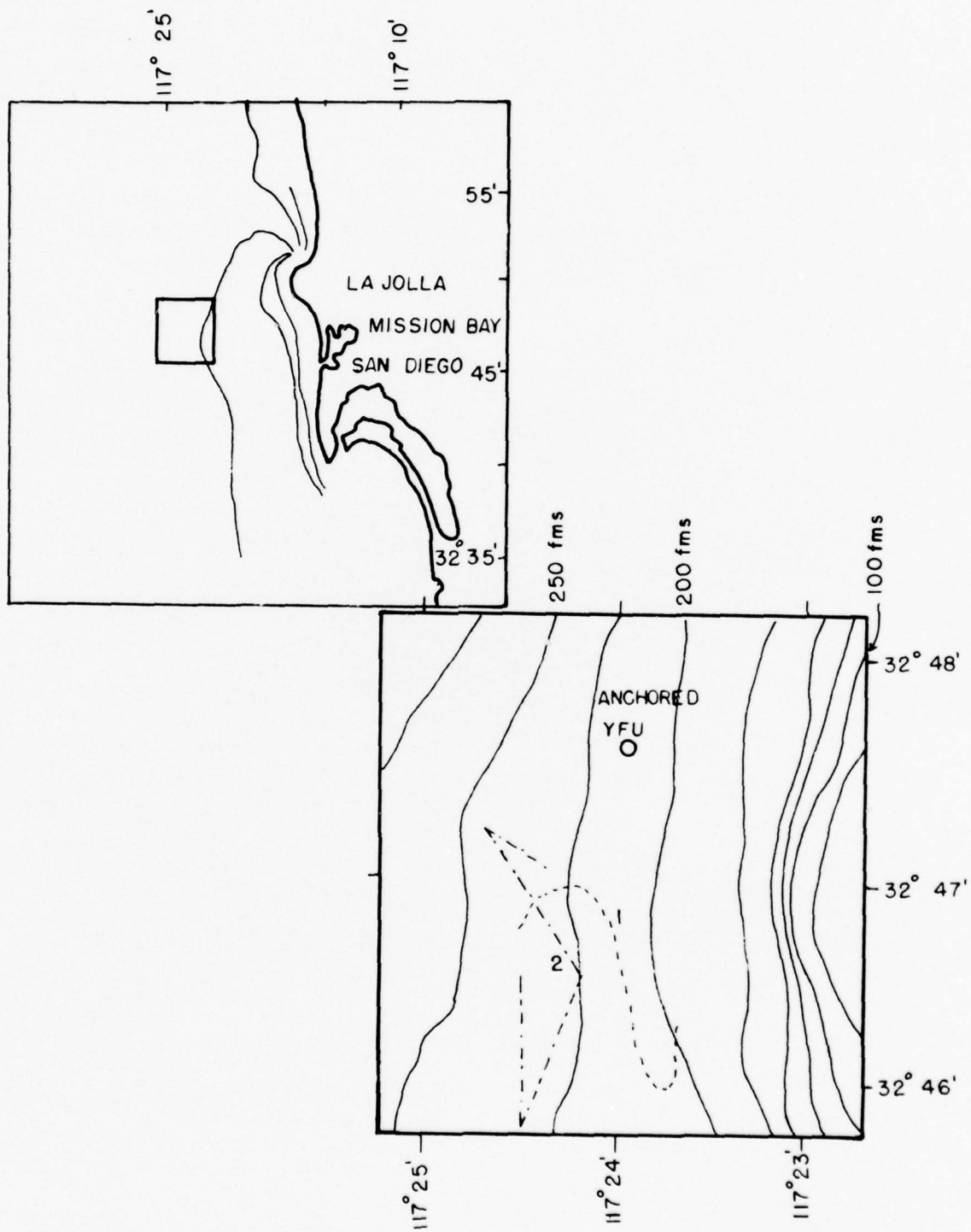


FIGURE 8. LOCATION OF TEST AREA (DOTTED LINES ARE TRACKS OF REXBURG DURING RUNS 1 AND 2)

anchoring of one or both vessels. Thus a stable point of reference is provided for the tests.

The sea bottom in this area consists of a layer of silty material of high porosity\* and low sound velocity, properties which are also characteristic of large areas in the deep Pacific Ocean basins.<sup>3</sup> Sound velocity in the upper part of this layer is close to or slightly less than that in the sea water near the bottom. As seen from Figure 9, sound rays striking the water-silt interface are partially reflected with the remainder of the energy going into the silt layer. If the silt layer is homogeneous this transmitted ray is refracted at the silt-water interface and follows a straight line path to the sub bottom where the energy is largely reflected and returns to the water along the path shown. The possible presence of a positive velocity gradient in the silt, uncertainty regarding the thickness of the silt, uncertainty regarding the roughness of the sub bottom, and uncertainty regarding the sound attenuation coefficient in the silt layer are complications which make it difficult to predict the reflection coefficient in this area.

Information obtained from the Sea Floor Study section of NEL<sup>10</sup> indicate that the bottom sediments are clayey silts approximately 7 yds thick over shale or sandstone. The physical and acoustic properties of the three media (water, silt, shale) are shown in Table I. An analysis of a sediment sample brought up by the anchor in this area is in agreement with the tabulated values. Also, recent in situ measurements obtained during a dive of the bathyscaph TRIESTE in this area provide

9

\*Ratio of the volume of voids (sea water) between the grains of a sediment sample to the total volume of the sediment.

WATER SURFACE

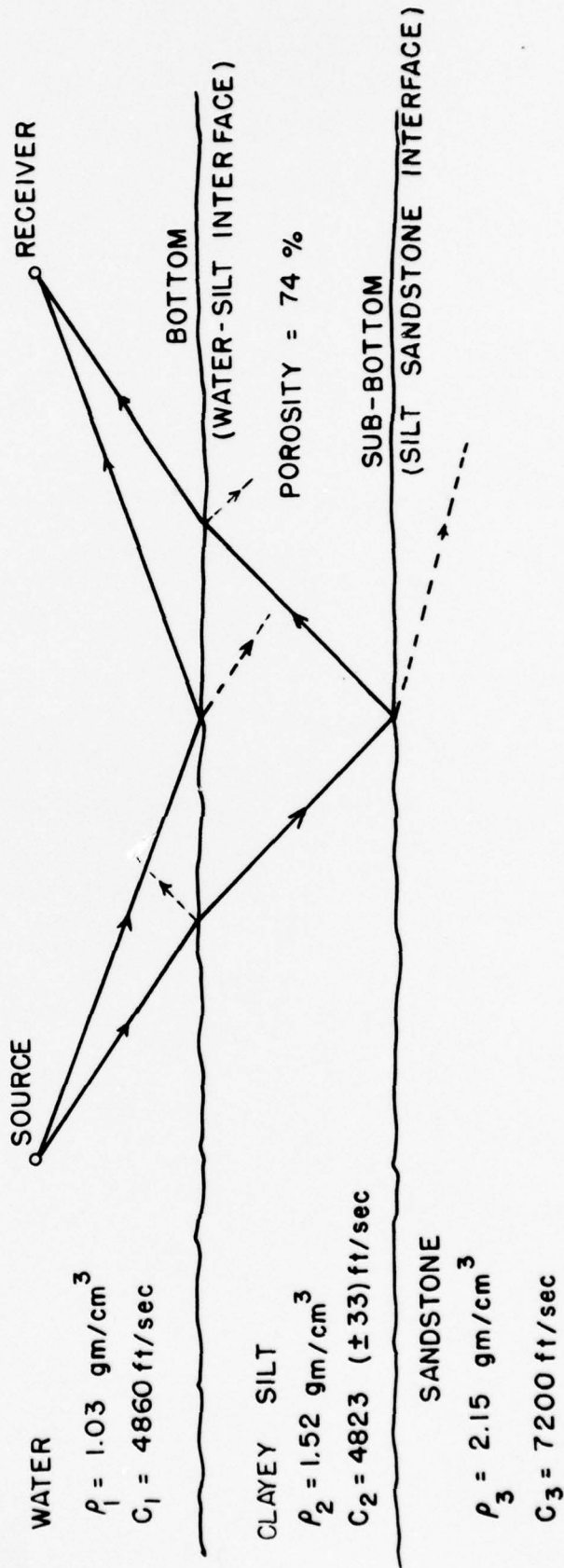


FIGURE 9. PHYSICAL PROPERTIES OF THE WATER AND SEDIMENT LAYERS IN THE TEST AREAS.

TABLE I  
 PHYSICAL AND ACOUSTIC PROPERTIES OF THE MEDIA

Medium	Density gm/cm <sup>3</sup>	Velocity km/sec	Attenuation db/m
Water	1.03	1.48	---
Silt	1.52	1.46-1.48	.004-.038
Shale	2.15	2.10-2.40	---

further confirmation for the water and silt sound velocities which appear in this table. During the dive of the TRIESTE acoustic probes were used to measure the sound velocity in the upper region of the silt. The sound velocity for the anchor sample was obtained from the porosity-sound velocity relationship described by Shumway.<sup>11</sup> The attenuation in the sediment was obtained from Shumway's<sup>11</sup> 30- to 37- kc/s values which were extrapolated to 1.5 kc/s. The average frequency dependence obtained from the 30- to 37-kc/s results may be expressed as,

$$\alpha = kf^{1.8} \dots \dots \dots (2)$$

where  $\alpha$  = attenuation in db,  $f$  = frequency, and  $k$  is the constant of proportionality. It is important to note that the average value of 1.8 has a standard deviation of approximately 1.0.

The properties of the third layer (shale or sandstone) are poorly known but this is less important than the other uncertainties already mentioned.

As already stated, the bottom in this area is fairly level and is believed to be quite smooth. In the October tests, for example, the tracks (Fig. 8.) were over bottoms which had fairly linear slopes of less than three degrees, as indicated by the echo-sounder aboard the REXBURG. Visual observations from the TRIESTE tend to confirm that the bottom is smooth, at least over the limited area seen through the viewport on the TRIESTE.

#### REDUCTION OF CW-PULSE DATA

The amplitude reflection coefficient for the ocean bottom is the ratio of the reflected sound-pressure amplitude to that of the incident sound wave. If path lengths are equal and the sound source and receiver are *omni*-directional this ratio can be found directly from the amplitude of the bottom-reflected and direct signals, such as those recorded on the Visicorder tape, Figure 4. At low grazing angles these conditions of path length and directivity were closely approximated. At other angles the ratio of the recorded amplitudes was corrected for difference in path length by assuming inverse square spreading.

Corrections for source and receiver directivity were obtained from the vertical directivity pattern seen in Figure 10. As this figure shows, the correction at low grazing angles (near  $90^\circ$ , Fig. 10) is small; in the neighborhood of  $45^\circ$  ( $135^\circ$ , Fig. 10) however the response is about 6 db down, which reduces the bottom-reflected amplitude by 12 db when both source and receiver are considered. The pattern in Figure 10 applies to the transducer on the YFU-45 as well as that on the REEBURG since they are of identical design. The hydrophones used are *omni*-directional at 1.5 kc/s.

Adjustments for difference in path length were made by assuming straight-line paths and applying an inverse-square spreading loss correction. At the small range difference involved, corrections for differences in absorption loss are negligible. Refraction effects which might produce shadow zones and invalidate the assumption of straight-line paths were considered of negligible importance because the velocity profile obtained during the tests shows only slight negative gradients at depths where low-grazing angles were considered. (See further discussion in a later section.) At higher grazing angles ( $25^\circ$  or greater) refraction

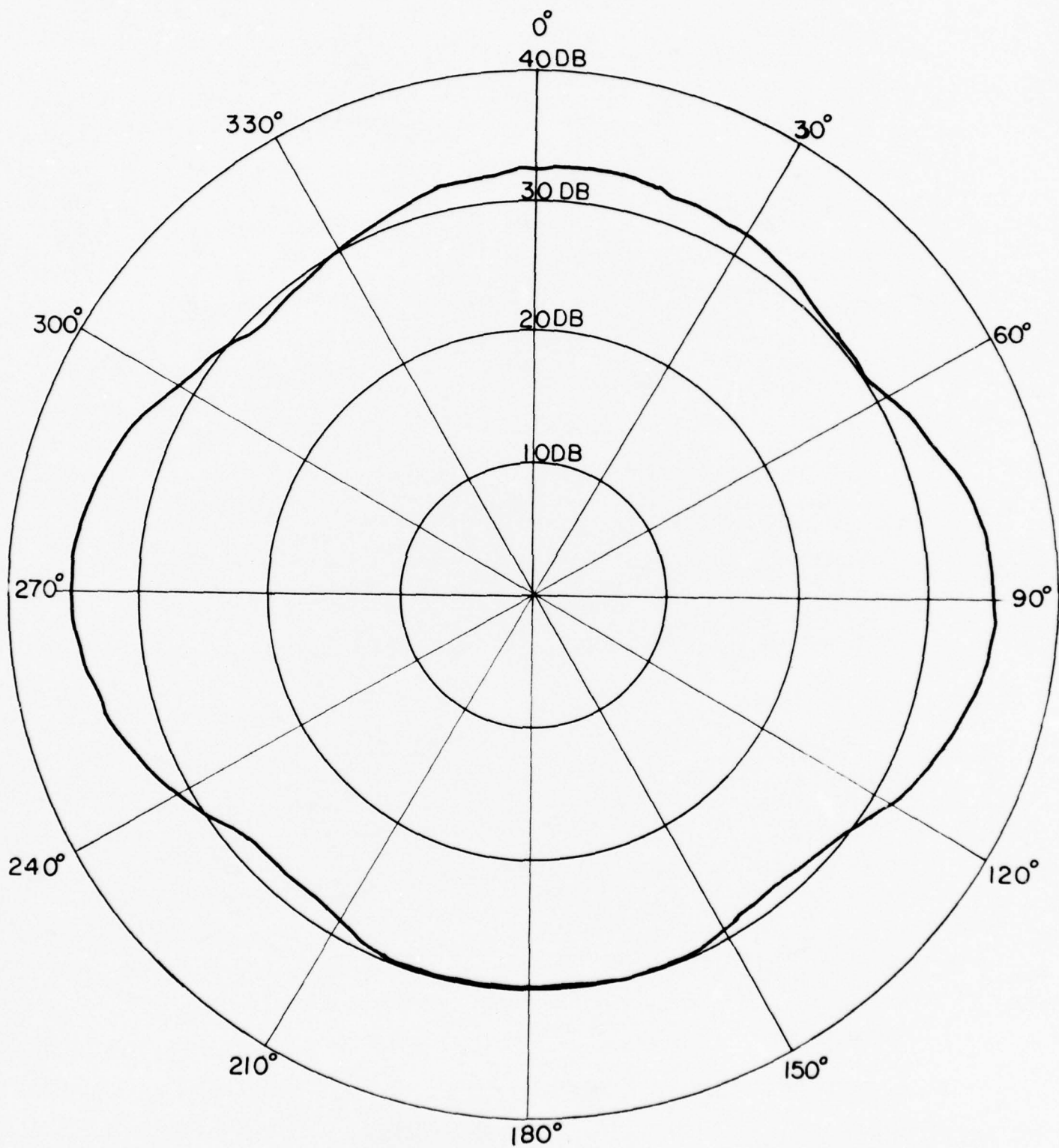


FIGURE 10. VERTICAL DIRECTIVITY PATTERN for B38CR3  
 TRANSDUCER AT 1.5 KC/S.

effects are negligible even when appreciable velocity gradients are present.

Path lengths and grazing angles were calculated by measuring travel time along the various paths using the radio pulse as a zero reference and the 200 cps signal as a time base. (See Fig. 4.) From these travel times and the average sound speed, as determined by the velocimeter, the path lengths and grazing angles could then be calculated. A velocity profile obtained in one of the velocimeter lowerings from the surface to the bottom, is reproduced in Figure 11.

#### RESULTS AND DISCUSSION

The individual amplitude reflection coefficients determined in the October tests are plotted in Figure 12 as a function of grazing angle. These unaveraged results present a somewhat unexpected picture. Although fluctuation is never unexpected in underwater sound research, that shown here seems to be excessive. In addition, the large number of reflection coefficients greater than unity was not anticipated. Under conditions where experimental control is considered good and in an area where the bottom appears to be smooth and produces a clean cut bottom reflected signal, with little evidence of distortion by excessive scattering, the results shown are somewhat surprising.

The data of Figure 12 is presented in a different, and perhaps less alarming, form in Figure 13. In this figure the average of all the coefficients in each 5-degree interval is plotted versus grazing angle. The standard error of a single observation is also indicated at each average value. The dotted line joining the average points now bears some resemblance to the decrease in reflection coefficient which might be expected from theory. The results seen in Figure 13 are

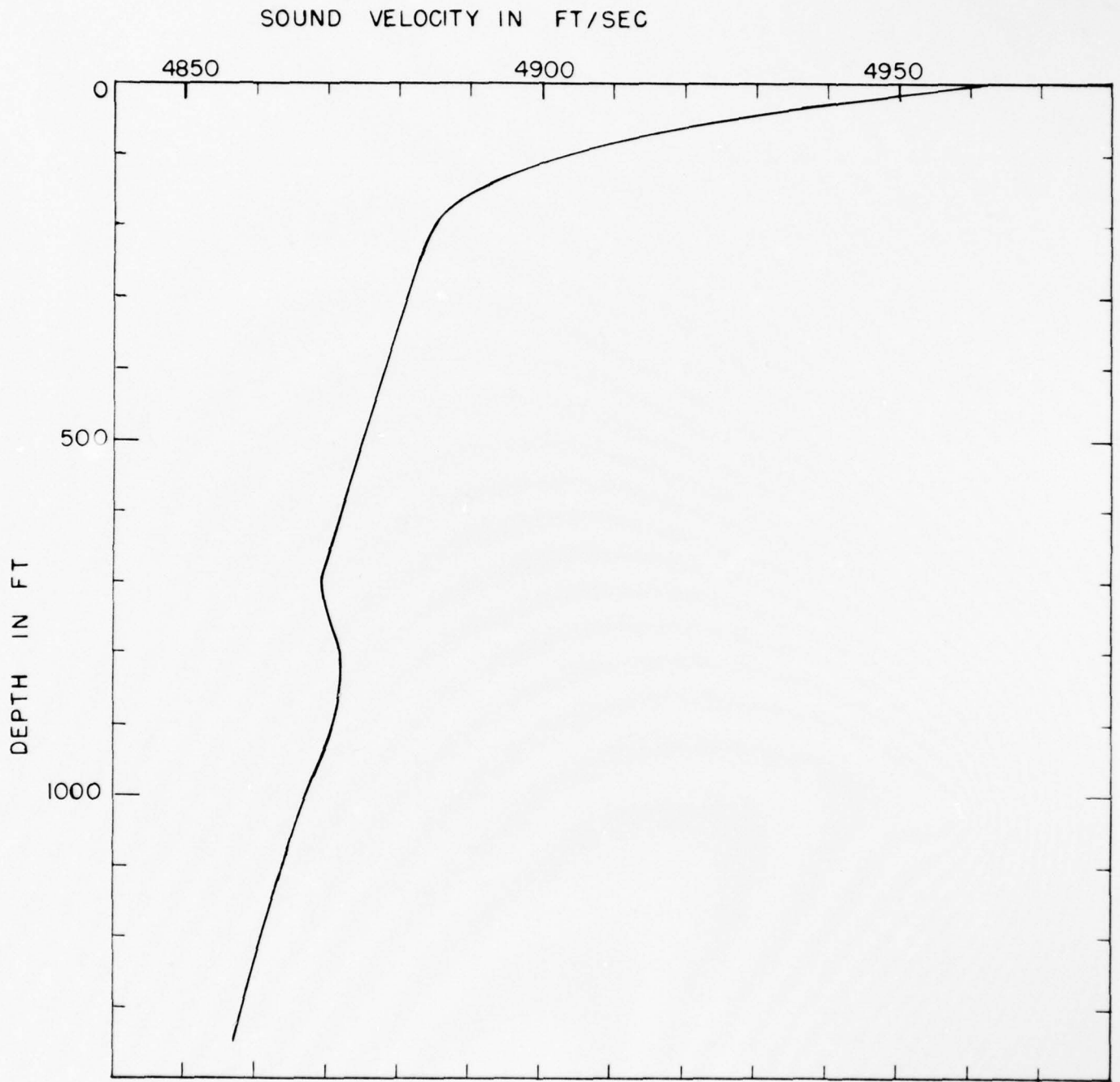


FIGURE II. SOUND VELOCITY PROFILE OBTAINED IN TEST AREA  
(OCTOBER 5, 1961)

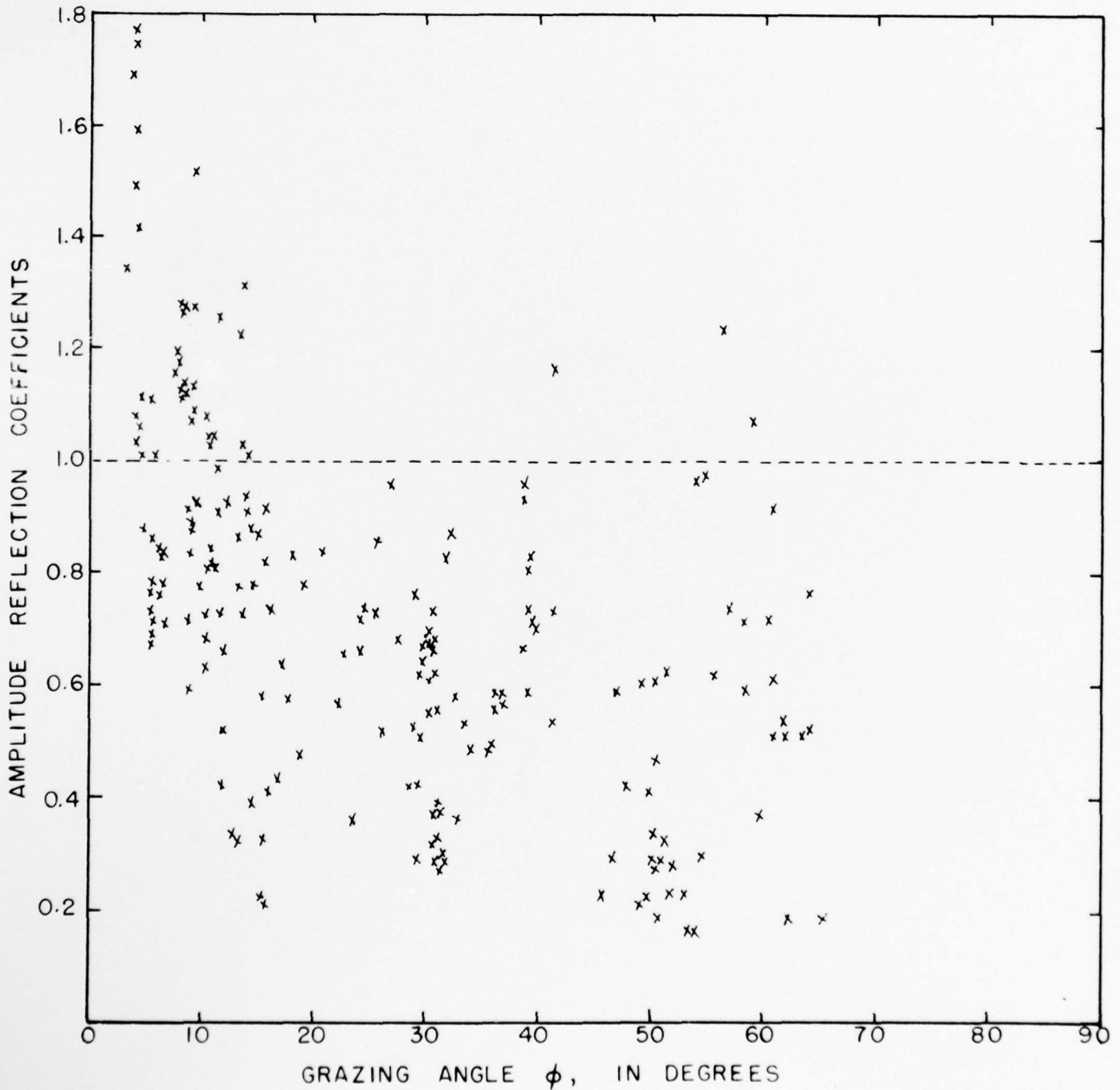


FIGURE 12. AMPLITUDE REFLECTION COEFFICIENTS AS A FUNCTION OF GRAZING ANGLE. (UNAVERAGED 5 MSEC. CW PULSE DATA FROM OCT. 1961 TRIP).

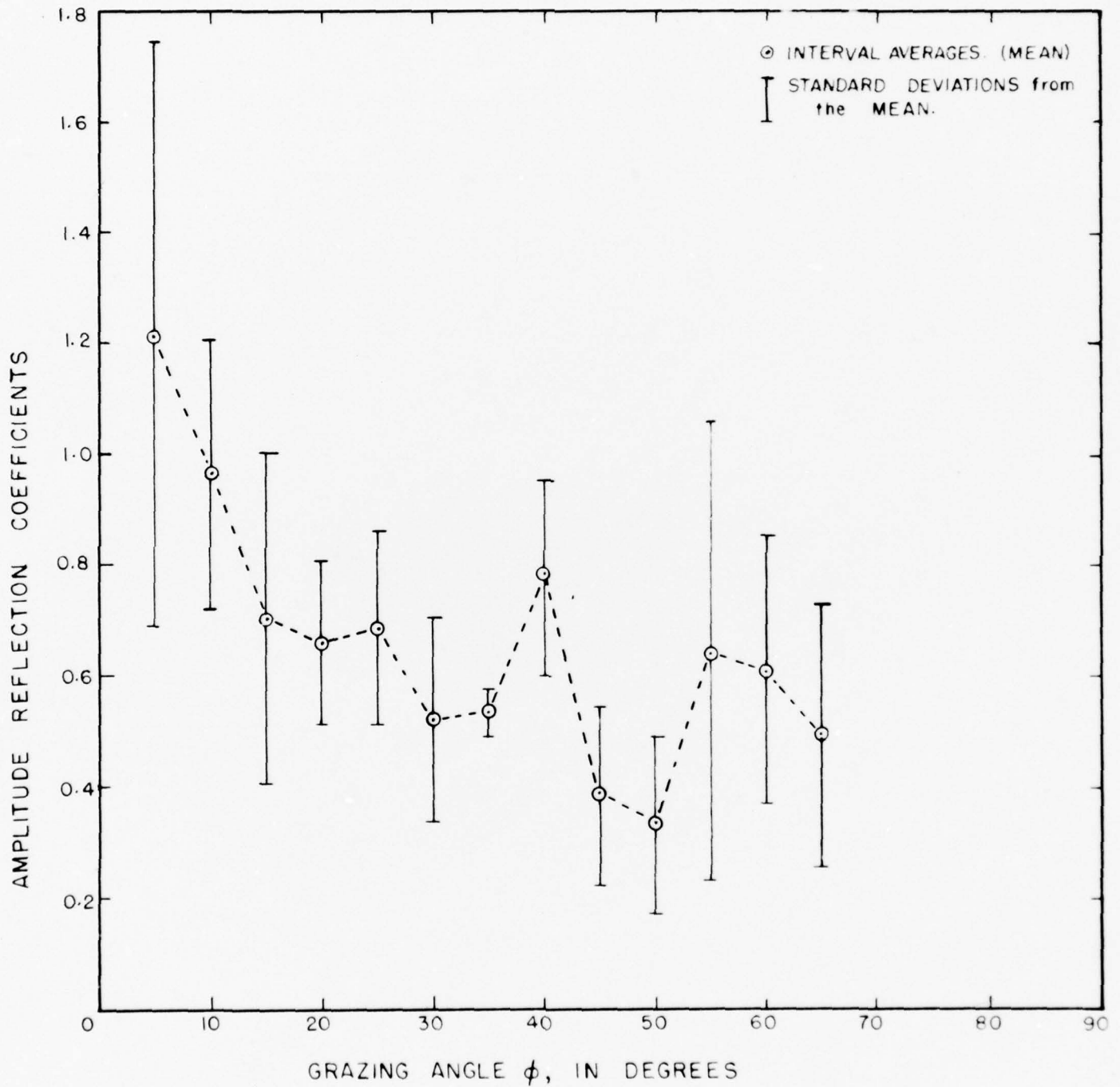


FIGURE 13. BOTTOM REFLECTION COEFFICIENTS (fig 12) AVERAGED OVER 5° INTERVALS.

also presented in Table II. In this table the reflection coefficients are listed according to receiver. Where 5 or more samples are available, fairly good consistency in reflection coefficient values from receiver to receiver was obtained. This provides some evidence regarding the effectiveness of the separate equipments but more samples are needed to give complete assurance. It is also obvious from the table that some regions ( $42.5^{\circ}$  to  $47.5^{\circ}$ , for example) have been poorly sampled.

Let us now examine some of the theoretical relations and compare their predictions with the results seen in Figure 13. The physical properties listed in Table I will be used as the basis for these predictions.

Figures 14 and 15 give the amplitude reflection coefficient curves that are obtained when a two layer model is assumed. Figure 14 shows the results obtained from the Rayleigh formula.<sup>1</sup> Since there is some doubt as to the precise value of the sound velocity in the clayey-silt layer, three curves were drawn. These three curves show the marked effect of slight variations in this parameter. The average values from Figure 13 are also plotted on Figure 14; these circled data points are well removed from all of the theoretical curves. Figure 15 presents the modified Rayleigh curves<sup>2</sup> using the same sets of physical properties as in the previous figure. The data points of Figure 13 again fall well above any of the theoretical curves for this two-layer model. It may seem obvious that the poor agreement between theory and experiment would occur, since we are actually concerned with a three-layer situation. However, since the attenuation in the silt layer, as well as the thickness of the layer and the type of material underlying it are poorly known,

TABLE II

## AVERAGE REFLECTION COEFFICIENTS BY RECEIVER

Angle	N*	YFU Deep Hydrophone	N	YFU Shallow Hydroph.	N	YFU Transducer	N	PCE Deep Hydrophone	N	PCE Transducer	N	Total
5					16	1.247			18	1.188	34	1.215 ±0.529
10	9	0.861			9	1.017	18	0.987	6	0.971	42	0.967 ±0.240
15	6	0.791	15	0.750			5	0.356	1	1.313	27	0.706 ±0.299
20	3	0.680	1	0.790			1	0.482			5	0.662 ±0.146
25	3	0.752	6	0.662							9	0.695 ±0.174
30	2	0.362	3	0.829	7	0.477	11	0.567	11	0.455	34	0.523 ±0.185
35	6	0.542			2	0.515					8	0.535 ±0.042
40	3	0.649	9	.825							12	0.761 ±0.175
45					2	0.450	1	0.227	1	0.422	4	0.386 ±0.162
50					5	0.488	7	0.221	6	0.336	18	0.332 ±0.154
55	4	0.831	1	1.247	1	0.298	1	0.153	1	0.164	8	0.646 ±0.412
60	6	0.553	5	0.689							11	0.613 ±0.243
65			3	0.411					1	0.763	4	0.497 ±0.239

\* N = number of samples

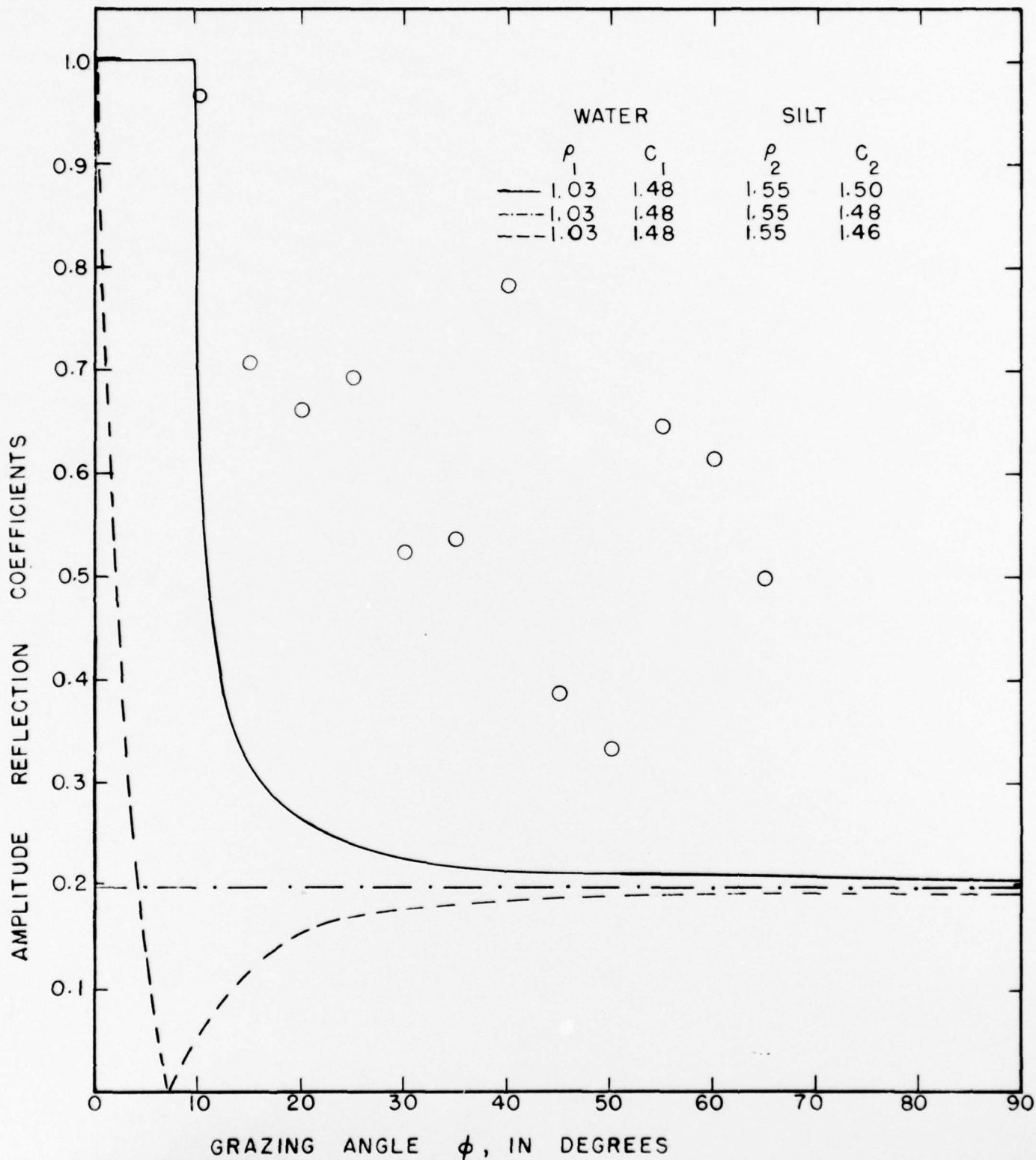


FIGURE 14. THEORETICAL AMPLITUDE REFLECTION COEFFICIENTS, RAYLEIGH FORMULA, TWO LAYER CASE.

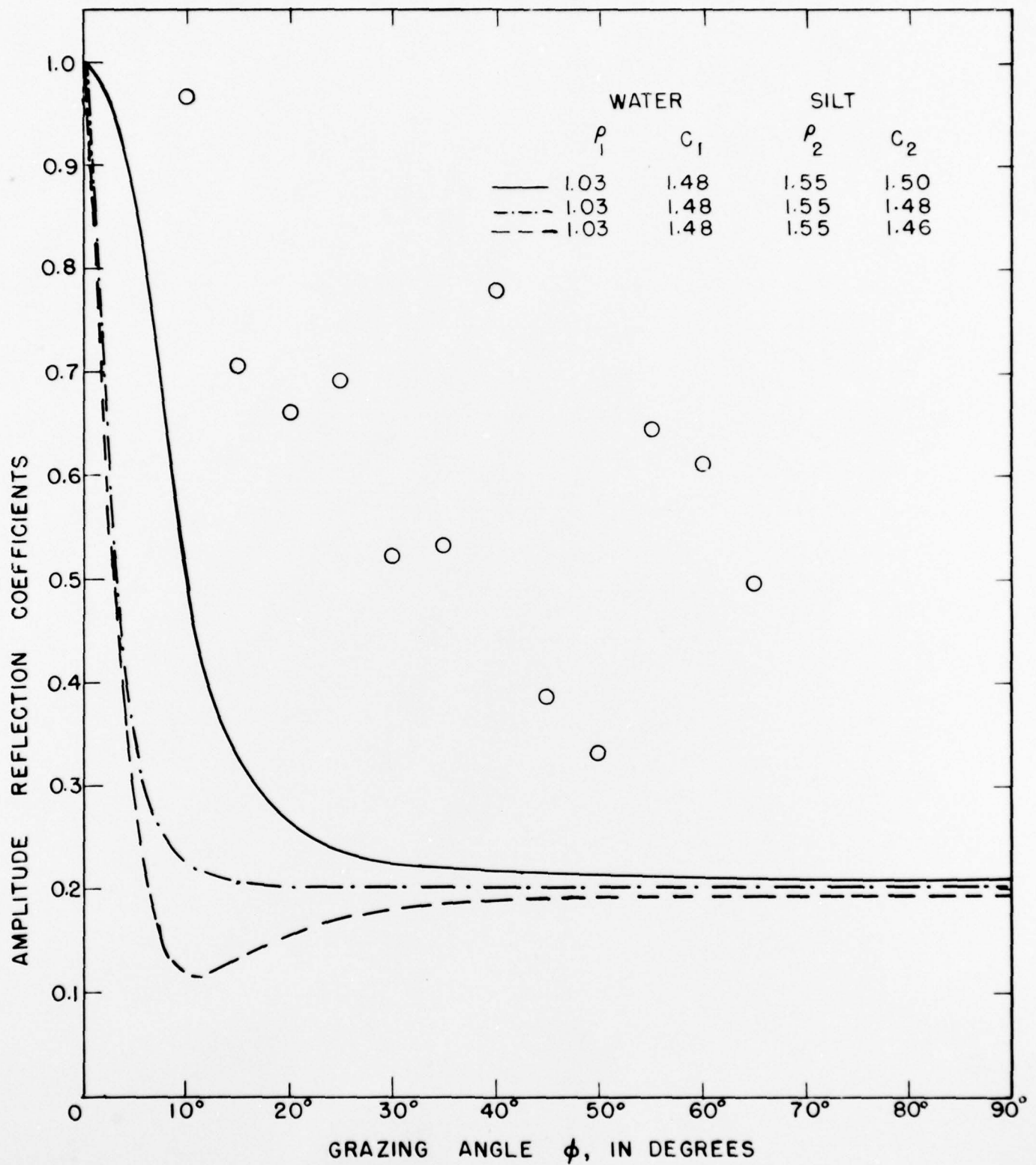


FIGURE 15. THEORETICAL AMPLITUDE REFLECTION COEFFICIENT, MODIFIED RAYLEIGH FORMULA, TWO LAYER CASE.

there was no assurance that any of the sound energy entering the silt would be returned to the water layer.

The poor agreement shown by the two-layer models has led to the trial of several three-layer models. The results from one such trial are shown in Figure 16. The procedure used in deriving these curves can be explained simply by referring to Figure 9. It is seen that the received signal may be considered as a combination of two signals, one arriving via a reflection at the water-silt interface, the other by a path through the silt layer with a reflection at the silt-sandstone interface. The signal which follows the second path will suffer losses at three boundaries as well as attenuation (absorption) losses in the silt layer. The unmodified Rayleigh<sup>1</sup> reflection and transmission relations were used to estimate the loss at each interface. The reflection coefficient curves seen in Figure 16 are derived from the resultant signal when the losses along the separate paths are considered and the two signals are added, powerwise at the receiver. An attenuation coefficient in the silt of .038 db/w was assumed in calculating each curve. Other parameters from Table I were used, as indicated on the figure, except that for the curve labelled  $C_1 < C_2$  a sound speed  $C_2 = 1.5$  km/sec was used. The averaged October data points have again been plotted on the figure; it is apparent that consideration of the three-layer model has resulted in a considerably improved fit.

The simplified model just considered is inadequate in some respects. For example, phase effects are not considered and the possibility of multiple reflection paths in the silt layer have been ignored.

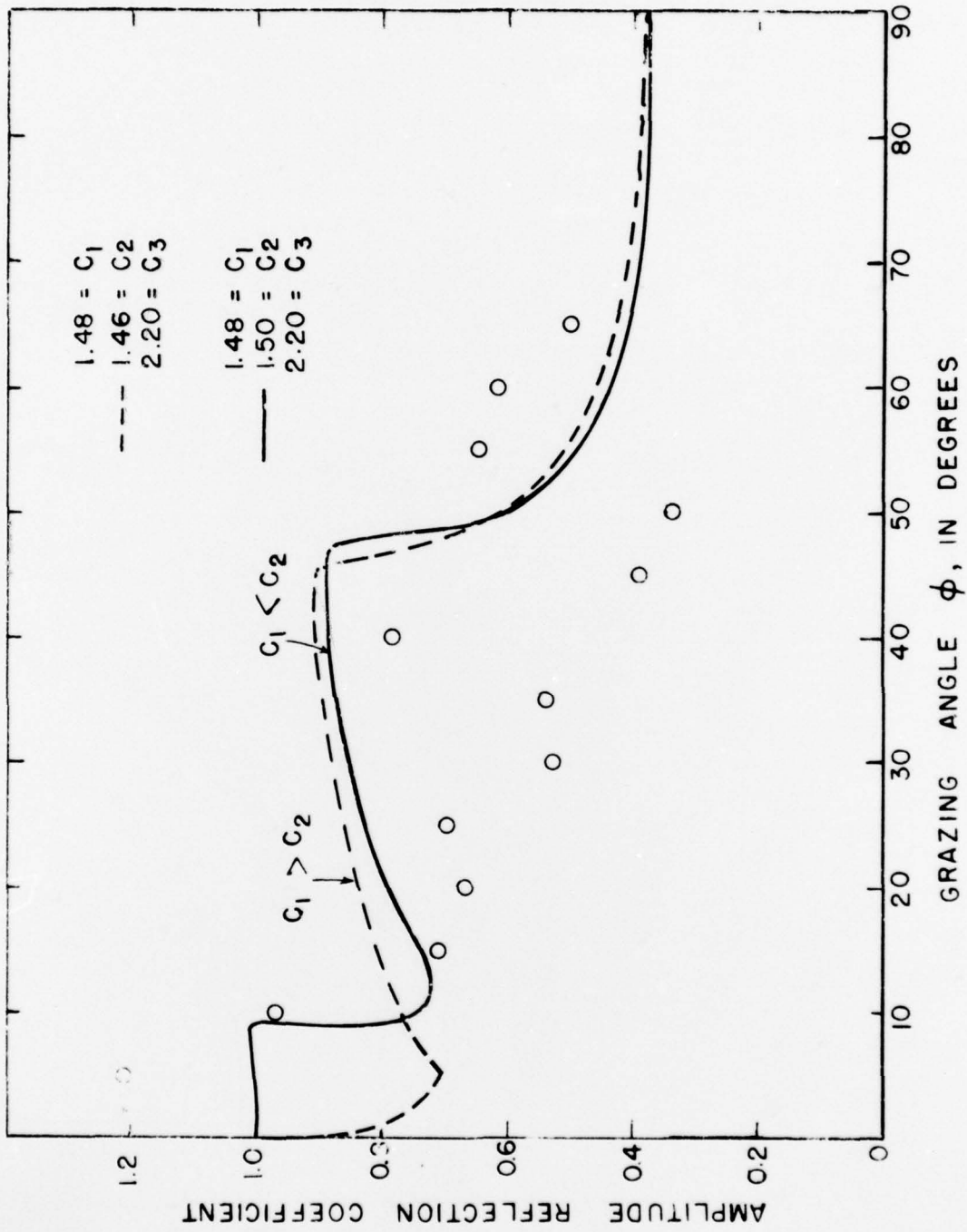


FIGURE 16. COMPOSITE RAYLEIGH CURVES OBTAINED BY COMBINING SIGNALS REFLECTED FROM BOTTOM AND SUB-BOTTOM.

The model suggested recently by Cole and Bell<sup>5</sup> cover these inadequacies and may provide a better fit to the data collected in this area. However, there are other possible mechanisms at work which may invalidate our assumptions, or which may be related to the large fluctuations and the high reflection coefficients which have been observed. Four of these mechanisms will be considered briefly.

(1) It is quite possible that a positive velocity gradient is present in the silt layer. If so the sound entering the layer would be refracted upward and could reenter the water layer without reaching the sandstone layer.

(2) The large number of observations in which the reflection coefficient has a value greater than unity has suggested the possibility of focusing. With both source and receiver essentially omni-directional and a bottom which is not a perfect plane surface it is possible to have sound reach the receiver by reflection at more than one point on the sea floor, and with little difference in path length. These individual signals could add vectorially to produce a highly variable signal.

(3) Another possible cause for the large number of coefficients greater than unity is that the direct arrival may be of lower amplitude than is predicted by inverse square spreading. To test this possibility the levels of the direct signals received on the transducers at the 1000 ft depth during an opening run of 2200 yds were plotted against range. The results obtained are shown in Figure 17. The plotted points in this figure scatter about the  $20 \log r$  spreading-loss line as the range increases from 800 to 2000 yds. In the region beyond 2000 yds, however, there is a marked decrease in level below that shown by the inverse-square spreading loss. As a result the reflection coefficients obtained

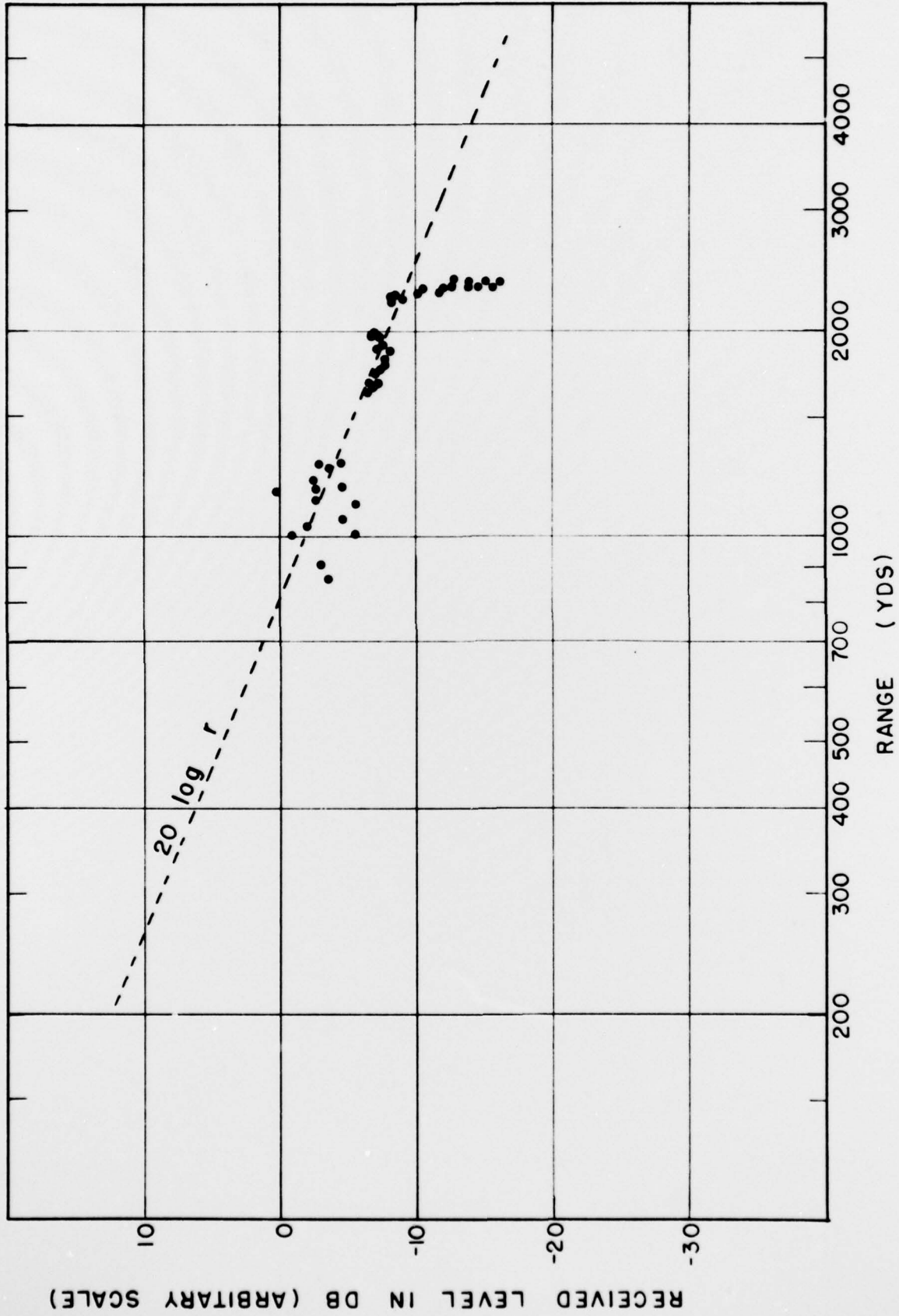


FIGURE 17. LEVEL OF DIRECT TRANSMISSION AS A FUNCTION OF RANGE.  
 (CW PULSES, TESTS 1, 2, 3,)

from this data are too high. It is believed that this accounts, in part at least, for some of the high values obtained in the low-angle region.

The droop in the level of the direct signal has been observed on several other runs at a critical range which seems to be associated with the distances of the source and receiver above the bottom. This has suggested the possibility that the decrease in signal may be caused by destructive interference between the direct signal and one which reaches the receiver by a refraction path,<sup>12</sup> as indicated in Figure 18. This path, EABH, goes from source to receiver via the silt-water interface and, for a velocity in the sediment greater than in the water, may reach the receiver at the same time as the direct signal. Thus interference would result, producing a lower (or higher) direct signal. Another possible refraction path follows the silt-shale interface ECDH. The critical range  $r_c$ , at which the direct and the refraction signal reach the receiver simultaneously is given by

$$r_c = 2Z \sqrt{\frac{c_2 + c_1}{c_2 - c_1}} \dots \dots \dots (3)$$

where  $Z$  is the distance of the source and receiver from the bottom and  $C_1, C_2$  are the sound velocities in the water and sediment, respectively. In the data and theory plot of Figure 16, the refraction path just discussed might very well lower the data point at 5 degrees grazing angle. Other data would not be affected.

In the example cited (Fig. 17) and several other cases, the critical range calculated from this expression falls close to the range where the level of the direct signal shows a marked departure from the 20 log  $r$  line. While further study of this possibility seems desirable there are a number

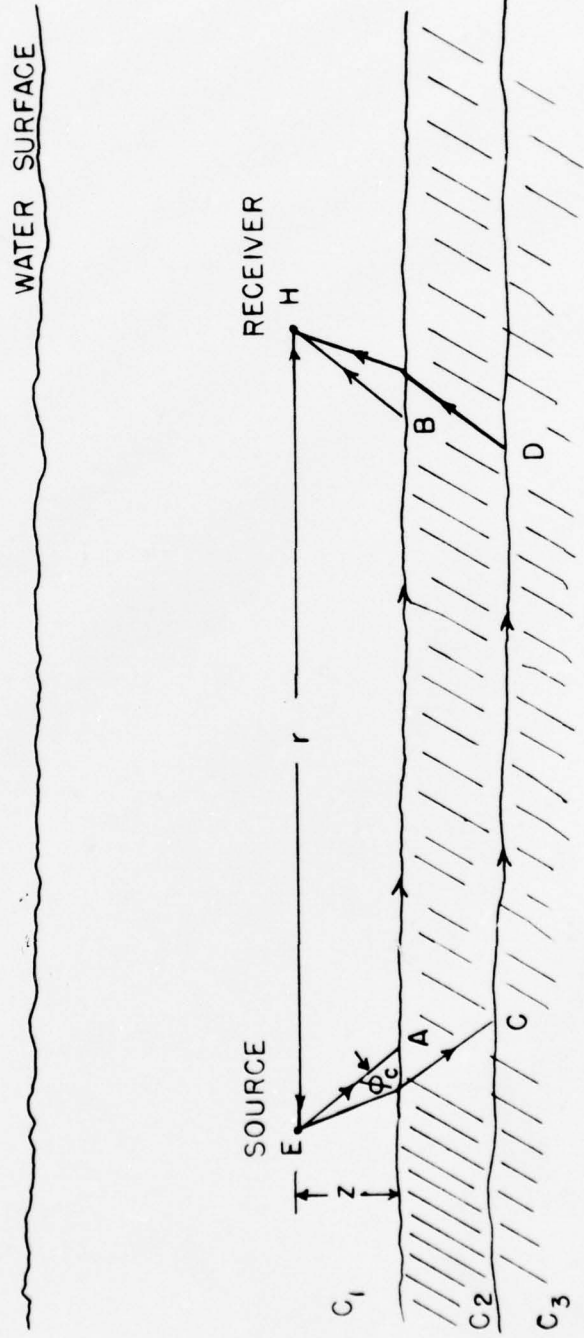


FIGURE 18. PATH OF THE REFRACTION WAVES ALONG THE WATER-SILT AND SILT-SHALE INTERFACE

of reasons why this explanation for the high (and low) coefficients at low grazing angles is an unlikely one. Of most importance, perhaps, is that considerable loss is expected in the sediment because of absorption and because the signal along the refraction path suffers an inverse fourth power loss. (See Ref. 1, p 196) Thus the signal via the refraction path may be of a relatively low level and may have little effect on the direct signal. This uncertainty can be clarified by resolving the refraction path signal. This has not been accomplished in the present data because ranges have not been great enough for this purpose. Resolution can also be accomplished by making  $Z$  in Equation (3) small; that is, by bringing the source and receiver closer to the bottom. Future tests will attempt to do this.

(4) The sudden decrease in the level of the direct signal seen in the graph (Fig. 17) could be caused by refraction effects such as those experienced if the receiver enters a shadow zone. For example, an unsuspected positive gradient near the bottom could create a shadow zone near the bottom similar to that commonly observed near the surface when a negative gradient is present. As already mentioned, refraction effects were considered negligible because velocity data, obtained from surface to bottom, had rather weak velocity gradients. This question has been checked further by constructing a ray diagram, Figure 19, based on the velocity profile of Figure 11. It is evident from this ray diagram that the source-to-receiver path at the 1000-ft level is but little affected by refraction and could not be responsible for the sharp drop in level seen at 2200 yds in Figure 17.

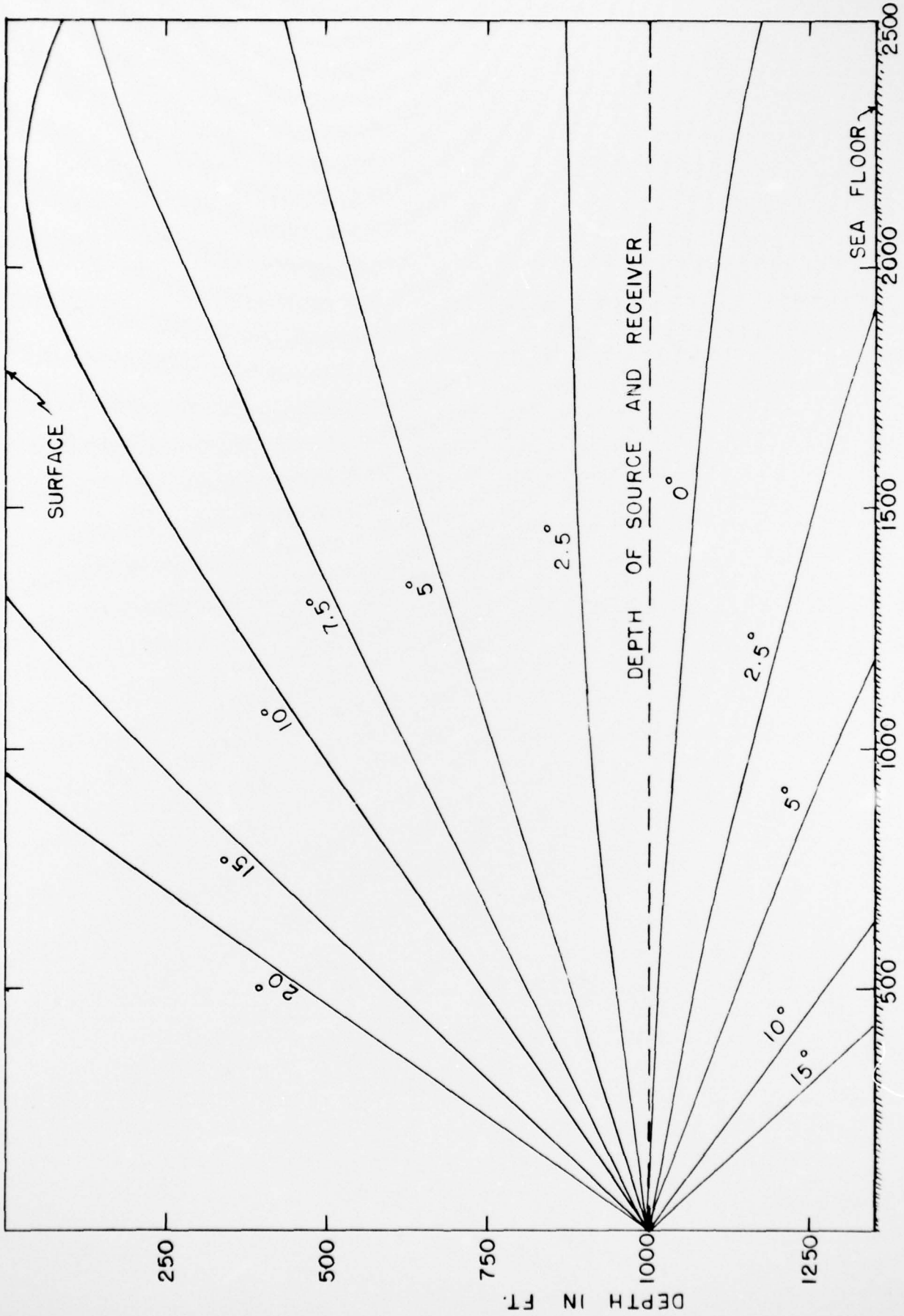


FIGURE 19. SOUND RAY DIAGRAM FOR 1000-FT SOURCE (BASED ON VELOCITY PROFILE FIG. II)

The authors conclude: (1)

#### CONCLUSIONS

1. The equipment used performed satisfactorily and appears to be adequate for further bottom-reflection loss tests.
2. <sup>A</sup> Of the signal types used, the CW pulses gave best results. The FM chirps have some advantages and their use will be continued. The linear FM pulses show promise for long-range, deep-water work but have no advantages at the ranges and depths used in this study; <sup>and (2)</sup>
3. The planned experimental procedure worked smoothly; with a few modifications it is adequate for our needs. In particular, it seems desirable to anchor both ships and vary the grazing angle by changing the depth of source and receiver. This procedure, with occasional changes in range, will give adequate grazing-angle coverage and will also provide a more stable experimental set-up.
4. <sup>></sup> The three-layer model applied to the October data gives a considerably better fit than any of the two-layer models. It is expected that better control of the experiment, better information on the physical properties of the sediment, more data with uniform coverage at all angles, and some changes in the three-layer model assumptions will remedy the disagreement still shown by the three-layer model.
5. The reason for the high fluctuations in reflection coefficient observed over many of the  $5^{\circ}$  intervals is not known. Although more data and better control will reduce this wide deviation it is believed that some unexplained mechanism such as focusing may be the chief cause.
6. The large number of reflection coefficients, at low grazing angles, with a value greater than unity is believed to result from an unexplained decrease in the level of the direct signal at a certain critical range.

Refraction effects do not appear to be the cause of this degradation in the direct signal. Interference between the direct signal and the refraction-path signal, that is, the signal which travels along the water-silt or silt-sandstone interface is suggested as a possible cause.

#### RECOMMENDATIONS

1. The low frequency bottom reflectivity studies should be continued. Only minor modifications in equipment and experimental procedure are needed.
2. An effort should be made to explain the abrupt attenuation of the direct signal which has been observed at certain critical ranges.
3. An investigation of the possible causes of the unexpectedly high fluctuation in reflection coefficients at a given angle should be made.
4. A better explanation of the experimental results by a more thorough examination of the three-layer model should be sought.
5. Tests over bottoms with a different and less complicated bottom structure is considered of major importance.
6. The use of other frequencies (10 kc and 3 kc) and explosive sources to give broad band coverage and to aid in resolving the various signal paths is recommended.

#### REFERENCES

1. Officer, C. B., Introduction to the Theory of Sound Transmission, p 76-78, McGraw-Hill 1958
2. Mackenzie, K. V., "Reflection of Sound from Coastal Bottoms", Journal of the Acoustical Society of America, v 32, p 221-231, February 1960
3. Fry, John C. and Russell W. Raitt, "Sound Velocities at the Surface of Deep Sea Sediments", Journal of Geophysical Research, Vol 66, No. 2, p 589, February 1961
4. Fry, J. C., "Reflection of Sound from the Deep Sea Floor", U. S. Navy Journal of Underwater Acoustics, v. 11, p 261-269, CONFIDENTIAL, April 1961
5. Cole, B. F. and T. G. Bell, "Three Layer Fluid Model for Ocean Bottom Reflectivity", Underwater Sound Laboratory, TM 905-55-62
6. Brekhovskikh, Leonid M., "Waves in Layered Media", p 50, Academic Press 1960
7. Lookingbill, D. C., "USS BAYA Instrumentation for 1956", p. IV-25 in Navy Electronics Laboratory Report 698, LORAD Summary Report, CONFIDENTIAL, 22 June 1956.
8. Liebermann, L. H., "Reflection of Sound from the Coastal Sea Bottoms", Acoustical Society of America, Journal, v 20, p 305-309, May 1948.
9. Liebermann, L. H., "Reflection of Underwater Sound from the Sea Surface", Acoustical Society of America, Journal, v 20, p 498-503, July 1948.
10. Hamilton, E. L. and others, "Acoustic and Other Physical Properties of Shallow-Water Sediments off San Diego", Acoustical Society of America Journal, v 28, p 1-15, January 1956

11. Shumway, G., "Sound Speed and Absorption Studies of Marine Sediments by a Resonance Method, Part II", *Geophysics*, v 25, p 659-682, June 1960.
12. Herring, C., "Transmission of Explosive Sound in the Sea", p 220-232 in National Defense Research Committee Division 6 Summary Technical Report v 8, Physics of Sound in the Sea, 1946